Available online at www.sciencedirect.com
ScienceDirect
Catalysis Today 125 (2007) 270–277
CATALYSIS TODAY
www.elsevier.com/locate/cattod

Effects of large pore zeolite additions in the catalytic pyrolysis catalyst on the light olefins production

Xianfeng Li [a,b,c], Baojian Shen [a,b,c,*], Qiaoxia Guo [c], Jinsen Gao [a,c,*]

[a] State Key Laboratory of Heavy Oil Processing, China University of Petroleum, Beijing 102249, PR China
[b] The Key Laboratory of Catalysis of China National Petroleum Corporation (CNPC), China University of Petroleum, Beijing 102249, PR China
[c] Faculty of Chemical Science and Engineering, China University of Petroleum, Beijing 102249, PR China

Available online 2 May 2007

Abstract

To increase the light olefins selectivity of catalytic pyrolysis catalyst for heavy oil processing, the effects of large pore zeolite additions on the selectivity to light olefins (ethylene and propylene) were studied in a micro-activity test (MAT) unit at 625 °C by using Daqing heavy oil and *n*-decene/*n*-decane as feedstocks. Rare earth containing ultra-stable Y, Hβ and four types of alkali-treated Hβ with different pore size distributions were employed as the large pore zeolite components. The yields of C_2–C_3 light olefins showed a volcano trend with the increasing amount of large pore zeolite additions. They reached up to 24.5 and 26.7 wt%, respectively, when an optimum combination of zeolites ZSM-5 and RE-USY or ZSM-5 and alkali-treated Hβ was used. Moreover, increasing the pore size of large pore zeolites also led to the increases in the yields of light olefins, the maximum total yields of ethylene and propylene reached up to 26.7 wt% when the total pore volume of the zeolite Hβ added was 0.452 $cm^3\ g^{-1}$.

Keywords: Heavy oil; Catalytic pyrolysis catalyst; Light olefins; Pore size

1. Introduction

Light olefins, such as ethylene and propylene, are very useful starting materials for chemical industry. It is known that the most important commercial light olefins production process is steam thermal cracking that uses light oils (such as naphtha and light cycle oil) or light hydrocarbons (such as ethane) as feedstocks. However, the worldwide increasing demand leads to the shortage of light oil supplies. Therefore, it is desirable that heavier feedstock be used in light olefins production. Under this circumstance, the DCC (deep catalytic cracking) process and the CPP (catalytic pyrolysis process) process have been successfully developed and commercialized by China Petroleum & Chemical Corporation (SINOPEC) [1,2]. The catalysts used in these processes play a very important role, and thus the research on olefin-selective zeolite-containing catalyst has received much attention [3].

Because of its outstanding hydrothermal stability and high selectivity to light olefins, ZSM-5 zeolite has been widely used as the active component of catalytic cracking catalyst [4]. Because of the limitation of pore size, however, a large number of higher hydrocarbon molecules cannot be cracked into the light olefins over ZSM-5 zeolite. Therefore, using large pore zeolites such as zeolite Y to crack these higher hydrocarbons into smaller hydrocarbon molecules and thus make them accessible to the pore structure of ZSM-5 zeolite is necessary [5–7]. On the other hand, catalyst pore size distribution has a significant influence on product selectivity [8]. Thus, two very interesting topics will be: (1) what is the ideal combination of ZSM-5 zeolite with large pore zeolites? (2) what is the appropriate pore size of large pore zeolites for a specific feedstock. Unfortunately, to the best of our knowledge, there is no report on this subject. In the present work, a RE-USY (rare earth containing ultra-stable Y zeolite) and a series of homemade β zeolites with different pore size distributions were employed as large pore zeolite components, and their effects on light olefins yields of ZSM-5 zeolite containing catalytic pyrolysis catalysts were investigated.

* Corresponding author. Tel.: +86 10 89733369; fax: +86 10 89733369.
E-mail address: baojian@cup.edu.cn (B. Shen).

0920-5861/$ – see front matter © 2007 Elsevier B.V. All rights reserved.
doi:10.1016/j.cattod.2007.03.021

2. Experimental

2.1. Materials

HZSM-5 ($n_{SiO_2}/n_{Al_2O_3}$ = 30, molar ratio), Naβ ($n_{SiO_2}/n_{Al_2O_3}$ = 25), Hβ ($n_{SiO_2}/n_{Al_2O_3}$ = 60) were commercially available products, RE-USY (framework $n_{SiO_2}/n_{Al_2O_3}$ = 8.58, RE_2O_3 = 0.97 wt%) was obtained from Lanzhou Petrochemical Company, PetroChina Company, Ltd. Zeolites β with different pore size distributions were obtained by alkali-treatment of Naβ ($n_{SiO_2}/n_{Al_2O_3}$ = 25) zeolite: firstly, zeolite Naβ was stirred in 0.1, 0.15, 0.2 and 0.25 M NaOH aqueous solutions at 80 °C for 90 min, respectively; then, the resulting slurries were filtered, washed and ion-exchanged; finally, they were calcined at 540 °C for 4 h to obtain the different alkali-treated Hβ zeolites named as AT-Hβ-1 to AT-Hβ-4, respectively.

2.2. Material characterization

2.2.1. X-ray diffraction and X-ray fluorescence

X-ray diffraction (XRD) patterns were recorded on a Shimadzu-6000 diffractometer that uses Cu Kα radiation and works at 40 kV, 30 mA, and a scanning rate of 2°/min. The molar SiO_2/Al_2O_3 ratios of the zeolites were determined by a Rigaku ZSX-100e X-ray fluorescence (XRF) spectrometer.

2.2.2. N_2 physisorption

The surface areas and pore size distributions of the samples were determined by N_2 physisorption using a Micromeritics ASAP 2020 automatic system. Each sample was degassed at 350 °C for 5 h prior to N_2 physisorption.

2.3. Catalyst preparation

The catalyst components (40 wt% (dry base) zeolites, 45 wt% (dry base) kaolin, and 15 wt% (dry base) alumina binder) were mechanically mixed to form a homogeneous slurry. The slurry was dried at 120 °C for 2 h and calcined at 540 °C for 4 h. The obtained solids were crushed to particles of 40–60 meshes (0.2–0.8 mm) and then aged with 100% steam at 750 °C for 6 h.

The catalyst series containing different amounts of RE-USY zeolite were named as Cat Y-0, Cat Y-1, Cat Y-2, etc. The catalyst series containing different amounts of AT-Hβ-4 zeolite were named as Cat B-0, Cat B-1, etc. The catalyst series containing the same amounts of alkali-treated Hβ zeolite (AT-Hβ) with different pore size distributions were named as Cat ATB-0, Cat ATB-1, etc. Moreover, the catalyst series containing different amounts of Hβ ($n_{SiO_2}/n_{Al_2O_3}$ = 60) zeolite were named as Cat HB-2, Cat HB-4. The compositions of the catalysts are listed in Tables 1 and 2, respectively.

2.4. Catalyst evaluation

The catalyst performance evaluation was carried out in a fixed-bed MAT unit designed according to ASTM D-3907. For each MAT test, the catalytic pyrolysis reaction was performed at 625 °C, contact time on stream 60 s, catalyst to oil ratio (wt/wt) 3.0, and WHSV 20 h^{-1}. During the reaction and stripping, liquid products were collected into a glass container kept in an ice bath. Gaseous products were collected into a gas burette by water displacement. The gaseous products and the liquid products were analyzed by gas chromatography, coke content on the catalysts was analyzed by a carbon analyzer. In all the testing experiments, the mass balance was controlled within 100 ± 5 wt%, and the yield of each fraction was calculated by mass normalization.

The feedstock used was a blend of 30 wt% Daqing vacuum tower bottom (VTB) and 70 wt% Daqing vacuum gas oil (VGO). The properties of the VTB and VGO are presented in Table 3.

n-Decene and *n*-decane were employed as the model compounds of naphtha range hydrocarbons to study the different cracking performances of alkene and alkane over the catalysts that use zeolites ZSM-5/β or ZSM-5/USY as active components.

3. Results and discussion

3.1. Catalyst design for light olefins production

It is well known that the structure of ZSM-5 consists of two types of 10-membered ring pore channels: straight channels of 0.53 nm × 0.56 nm and cross-linked sinusoidal channels of 0.51 nm × 0.55 nm [9]. Therefore, the ZSM-5 type zeolites can perform as a shape-selective catalytic component. It is reasonable to conceive that increasing the light olefins selectivity and yields of a catalyst can be achieved by increasing the accessibility of hydrocarbons to the olefin-selective zeolite ZSM-5. However, many large hydrocarbon

Table 1
Compositions of the catalyst series containing different amounts of RE-USY zeolite or Hβ zeolite

Catalyst	Y-0(B-0)	Y-1	Y-2	Y-3	Y-4	B-1	B-2	B-3	B-4	HB-2	HB-4
Zeolites (wt%)											
HZSM-5	40	30	20	10	–	30	20	10	–	20	–
RE-USY	–	10	20	30	40	–	–	–	–	–	–
AT-Hβ-4	–	–	–	–	–	10	20	30	40	–	–
Hβ (60)	–	–	–	–	–	–	–	–	–	20	40
Kaolin (wt%)	45	45	45	45	45	45	45	45	45	45	45
Alumina binder (wt%)	15	15	15	15	15	15	15	15	15	15	15

Table 2
Compositions of the catalyst series containing Hβ zeolites with different pore size distributions after alkali-treatment

Catalyst	ATB-0	ATB-1	ATB-2	ATB-3	ATB-4(B-2)
Zeolites (wt%)					
HZSM-5	20	20	20	20	20
Hβ (25)	20	–	–	–	–
AT-Hβ-1	–	20	–	–	–
AT-Hβ-2	–	–	20	–	–
AT-Hβ-3	–	–	–	20	–
AT-Hβ-4	–	–	–	–	20
Kaolin (wt%)	45	45	45	45	45
Alumina binder (wt%)	15	15	15	15	15

molecules cannot be directly cracked into light olefins over ZSM-5 zeolite, one possible way to realize this is to add a relatively large pore zeolite to ZSM-5 zeolite. To design such a catalyst, two types of zeolites, RE-USY and Hβ, were chosen as the large pore zeolites of the catalytic pyrolysis catalyst to be developed.

n-Decane and *n*-decene were used as probe molecules to evaluate the designed catalyst. The yields of light olefins (ethylene and propylene) versus the catalyst composition are shown in Fig. 1, and the conversion data versus the catalyst composition are shown in Fig. 2.

Fig. 1 indicates that at the same conversion, the ZSM-5-based catalyst shows higher selectivity to light olefins compared with the RE-USY or β-based ones and the combined RE-USY and ZSM-5 or Hβ and ZSM-5-based ones for both of the two feedstocks. However, Fig. 2 reveals that a higher conversion can be obtained by employing the large pore zeolite RE-USY or β when *n*-decane was used as the feedstock. Moreover, the evaluation results indicate that the combination of Hβ zeolite and ZSM-5 zeolite gives the better result than that of RE-USY zeolite and ZSM-5 zeolite. When *n*-decene was used as the feedstock, there is no obvious difference in conversion for all the cases, since the conversion is very high under the selected condition (at 625 °C). The above results indicate that for higher yields of light olefins, both shape-selective zeolite ZSM-5 and the large pore zeolite RE-USY or β are important. ZSM-5 zeolite increases the selectivity to light olefins, and the large pore zeolites (RE-USY and β zeolites) are favorable for increasing the conversion.

Table 3
Properties of Daqing VTB and VGO

Parameters	VTB	VGO
Density (20 °C) (g/cm^3)	0.93	0.87
Viscosity (100 °C) (mm^2 s^{-1})	137.67	11.28
Carbon residue (wt%)	8.22	0.30
IBP (°C)	456	423
Distillation cut (500 °C) (wt%)	7	38
Elemental analysis (wt%)		
C	87.03	86.30
H	12.67	13.70
N	0.30	0

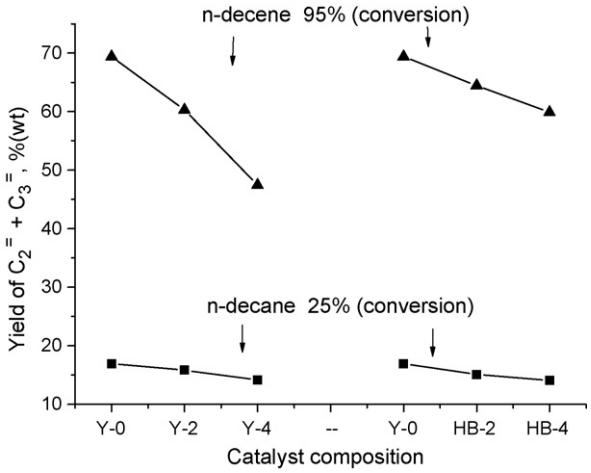

Fig. 1. Yields of ethylene and propylene vs. catalyst composition at the same conversion.

3.2. Pore structure of the alkali-treated Hβ zeolite and its effect on light olefins selectivity

In order to study the influence of different pore size distributions of the same type of zeolites on light olefins yield, an alkali-treatment method was employed to treat β zeolite to obtain four different AT-Hβ zeolites.

Fig. 3 presents the XRD patterns of the β zeolite samples between 5° and 45°. From these results, it is concluded that after the alkali-treatment the basic structure was well reserved.

It is known that during the alkali-treatment the silicon species in zeolite structure were reacted with alkali and partly extracted by the alkali solution from the original zeolite crystals [10]. In the present experiment, Naβ zeolite crystals were allowed to react with the alkali aqueous solution, the framework of zeolite β was partly dissolved, providing the opportunity to form extra macro- and/or meso-pores and cavities. When the Naβ zeolite was treated with the NaOH alkali solutions of different concentration, the amounts of silicon species dissolved were different, giving rise to the different pore distributions.

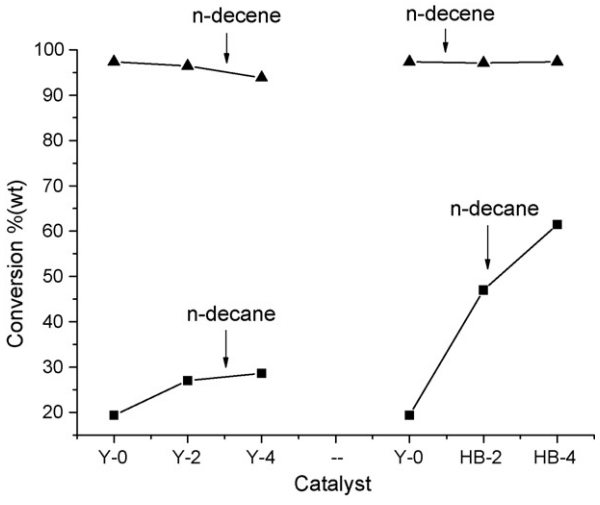

Fig. 2. The change of conversion on different catalysts.

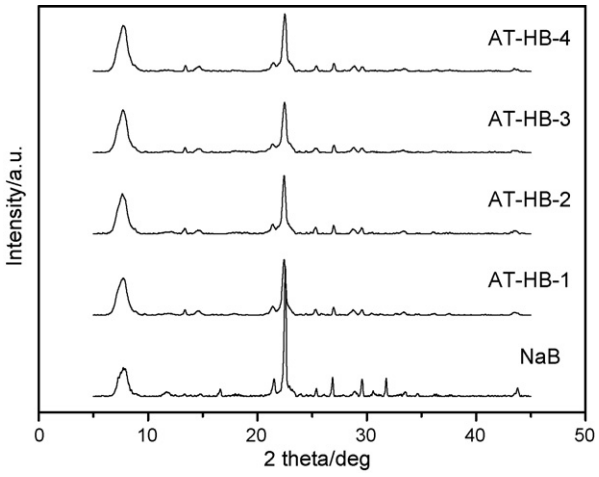

Fig. 3. XRD patterns of as-received Naβ and AT-Hβ zeolites.

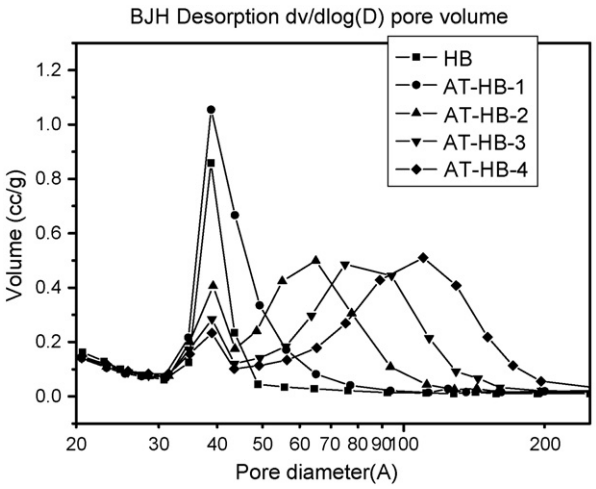

Fig. 5. Pore size distributions of the different kinds of zeolite β.

The nitrogen adsorption–desorption isotherms of the AT-Hβ zeolites are shown in Fig. 4. The isotherms of the AT-Hβ zeolites (such as AT-Hβ-2, AT-Hβ-3 and AT-Hβ-4) clearly show steep hysteresis loops, indicating the presence of meso-pores. A partial dissolution of silicon and alumina species in the zeolite framework causes the enlargement of micropores, resulting in the formation of meso-pores in the Naβ zeolites. The relative pressure (P/P_0), at which the hysteresis loops appear, increases in the order of AT-Hβ-1 < AT-Hβ-2 < AT-Hβ-3 < AT-Hβ-4, indicating the increasing pore size. Most possibly, the amount of micropores was considerably decreased and the pore size of meso-pores increases gradually with the increasing alkali concentration. The large hysteresis loops in these isotherms also confirm the formation of meso- and macro-pores. Moreover, the nitrogen adsorption isotherms show a climbing trend, indicating that the diameters of the Naβ zeolite particles were gradually decreased with the increasing alkali concentration.

Fig. 5 shows the pore size distribution profiles of the different zeolite β samples obtained by using the N_2 sorption/desorption method. It can be seen that the pore diameters of the AT-Hβ zeolites obviously increased with the increasing concentration of the NaOH alkali solutions. After the different alkali treatments, in addition to some amorphous silica and alumina, the structural units are also partly dissolved, forming partial extra macro- and/or meso-pores and cavities, so the micropore areas of the β zeolites were quickly decreased from 419 $m^2\ g^{-1}$ to 379 $m^2\ g^{-1}$, and the external surface areas were gradually increased from 117 $m^2\ g^{-1}$ to 149 $m^2\ g^{-1}$. Moreover, the total pore volumes and mesopore volumes were increased from 0.328 $cm^3\ g^{-1}$ to 0.452 $cm^3\ g^{-1}$ and from 0.109 $cm^3\ g^{-1}$ to 0.254 $cm^3\ g^{-1}$, respectively. Furthermore, the average pore diameter can reach up to 34.2 Å from the original 24.5 Å. The textural data of the samples are listed in Table 4, in which the textural data of the zeolites RE-USY and Hβ ($n_{SiO_2}/n_{Al_2O_3}$ = 60) are also presented.

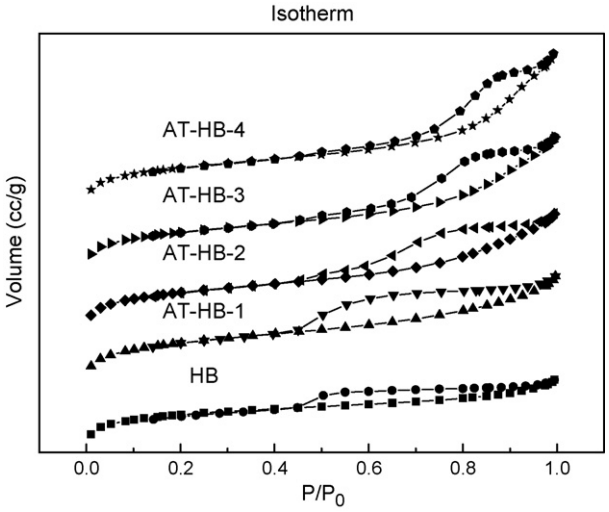

Fig. 4. N_2 adsorption–desorption isotherms of the different kinds of zeolite β.

The relative crystallinity data of the AT-Hβ zeolites are presented in Table 5. Because an alkali solution can partially destroy the structure of β zeolite, the relative crystallinity of all the AT-Hβ zeolites was decreased in different degrees compared with that of the original Naβ zeolite. However, during the alkali-treatment, the structural unit was only partly destroyed, but was not completely extracted by the low concentration alkali solution. The amounts of the dissolved silicon species from destroyed structural units increased with the increasing alkali solution concentration. Moreover, some amorphous silica and alumina among the interstices of the β zeolite crystals were also dissolved when the concentration of the alkali solution was high enough, leading to that the mixed crystal structure of the β zeolite was slowly desquamated, and therefore the diameter of the β particles was decreased, which can also be proven by the adsorption–desorption isotherms of nitrogen. M. Ogura et al. [10] observed that silicon species were dissolved from relatively weaker parts of ZSM-5 zeolite such as growing faces, resulting in the better crystallinity of the remaining zeolite. In the present work, it was observed that the relative crystallinity was gradually increased with the increasing alkali solution concentration.

Table 4
The textural data of the zeolite samples

Sample	S_{BET} ($m^2\ g^{-1}$)	S_{micr} ($m^2\ g^{-1}$)	S_{exte} ($m^2\ g^{-1}$)	V_P ($cm^3\ g^{-1}$)	V_{micr} ($cm^3\ g^{-1}$)	V_{meso} ($cm^3\ g^{-1}$)	Average pore diameter (Å)
Hβ-0	536	419	117	0.328	0.219	0.109	24.5
AT-Hβ-1	546	415	131	0.396	0.217	0.179	27.8
AT-Hβ-2	530	382	149	0.395	0.199	0.196	29.8
AT-Hβ-3	522	376	146	0.418	0.197	0.221	32.0
AT-Hβ-4	528	379	149	0.452	0.198	0.254	34.2
RE-USY	539	462	77	0.376	0.241	0.136	27.9
Hβ (60)	441	345	95	0.302	0.180	0.121	27.4

Table 5
The relative crystallinity of AT-Hβ zeolites before and after hydrothermal treatment

Zeolite	Relative crystallinity (%)/before hydrothermal treatment	Crystallinity loss (%)	Relative crystallinity (%)/after hydrothermal treatment	Crystallinity loss (%)
AT-Hβ-1	75	25	72	28
AT-Hβ-2	80	20	73	27
AT-Hβ-3	90	10	80	20
AT-Hβ-4	92	8	86	14

Notes: (1) The crystallinity (%) of the as-received Naβ zeolite was defined as 100%; (2) the zeolites were hydrothermally aged in 100% steam at 750 °C for 6 h.

Similar to other zeolites, the hydrothermal treatment can affect the crystallinity of the AT-Hβ zeolites. After the hydrothermal treatment, the crystallinity of the AT-Hβ zeolites was decreased in different degrees. The results are also presented in Table 5. Moreover, a part of the textural data of the zeolite samples before and after the hydrothermal treatment are presented in Table 6. Their total surface areas were decreased, but total pore volumes were increased.

Moreover, during the alkali-treatment, silicon species were selectively dissolved from the framework of the zeolite β, resulting in the decrease in the molar SiO_2/Al_2O_3 ratio of the zeolite β. The molar SiO_2/Al_2O_3 ratios of the original β zeolite and the AT-Hβ zeolites are presented in Table 7. It can be seen that the molar SiO_2/Al_2O_3 ratios of the β zeolites decreased with the increasing alkali concentration.

In order to determine the effect of the AT-Hβ zeolites on light olefins selectivity, the Hβ zeolite and AT-Hβ zeolites were employed to make the ATB-X catalyst series. The effect of the additions of the different AT-Hβ zeolites on product yields is presented in Table 8.

The experimental results indicate that the large pore zeolite additions can effectively increase the yield of light olefins (ethylene and propylene). Fig. 5 and Table 8 show that the increasing pore size of the large pore zeolites in the order of Hβ, AT-Hβ-1 to AT-Hβ-4 also results in the continually increasing yields of ethylene and propylene. The maximum total yield of ethylene and propylene reached at 26.7 wt% when the total pore volume of the large pore zeolite added was 0.452 $cm^3\ g^{-1}$. It was found that the yield of light olefins increased by 7.2 wt% compared with the case using the Hβ zeolite as large pore zeolite. It can be explained that the increasing pore size of the AT-Hβ zeolites favors mass transfer and leads to more efficient cracking of large hydrocarbon molecules into C_2–C_3 light olefins.

From Fig. 6, it can be seen that the yield of propylene also increases with the increasing pore size of the AT-Hβ zeolites added. The possible reasons are: firstly, over the catalysts containing the zeolites with meso- and macro-pores formed during the alkali-treatment, further oligomerization and cracking are suppressed by the rapid elution of the primary cracking products, and thus high selectivity to propylene becomes possible [11]; secondly, the catalysts with large pores favor the bimolecular reaction mechanism that may be beneficial to producing more propylene from the feed that mainly includes monobranched hydrocarbons [12].

Moreover, it is well established that zeolite pore structure can significantly impact the rate of coke formation in a number of acid-catalyzed reactions [13]. Catalysts ATB-1 to ATB-4 showed a slightly higher coke yield (from 1.0 wt% to 1.6 wt%)

Table 6
The textural data of the zeolite samples before and after hydrothermal treatment

Sample	S_{BET} ($m^2\ g^{-1}$)	S_{micr} ($m^2\ g^{-1}$)	S_{exte} ($m^2\ g^{-1}$)	V_P ($cm^3\ g^{-1}$)	V_{micr} ($cm^3\ g^{-1}$)	V_{meso} ($cm^3\ g^{-1}$)	Average pore diameter (Å)
Hβ-0-B	536	419	117	0.328	0.219	0.109	24.5
Hβ-0-A	454	362	91	0.333	0.178	0.156	29.4
AT-Hβ-3-B	522	376	146	0.418	0.197	0.221	32.0
AT-Hβ-3-A	425	271	154	0.436	0.126	0.310	41.0

Notes: (1) The zeolites were hydrothermally aged in 100% steam at 750 °C for 6 h; (2) "B" expresses the sample before hydrothermal treatment; (3) "A" expresses the sample after hydrothermal treatment.

Table 7
The molar SiO_2/Al_2O_3 ratios of the original β zeolite and AT-Hβ zeolites

Zeolite	SiO_2/Al_2O_3
Naβ	25.69
AT-Hβ-1	23.23
AT-Hβ-2	22.17
AT-Hβ-3	21.12
AT-Hβ-4	20.76

Table 8
Product yields (wt%) on the ATB catalyst series

Product yields	Catalyst				
	ATB-0	ATB-1	ATB-2	ATB-3	ATB-4
Dry gas	12.9	11.6	13.4	13.5	12.4
Liquid gas	39.0	40.0	36.2	38.9	40.7
Liquid	42.9	41.6	43.8	41.4	40.6
Coke	5.2	6.8	6.7	6.2	6.3
Ethylene	5.8	5.4	6.3	6.2	6.6
Propylene	13.6	16.7	17.2	17.7	20.1
Ethylene + propylene	19.5	22.1	23.6	23.9	26.7

compared with catalyst ATB-0. This may be attributed to the steric limitations of smaller micropores to hinder the formation of the hydrogen transfer transition state [14]. Meanwhile, it is interesting to note that the coke yields of catalysts ATB-1 to ATB-4 tend to decrease, possibly due to the acidity change of the AT-Hβ zeolites. The alkali-treatment of the Naβ zeolite induced the dissolution of silica, resulting in the decrease in the molar SiO_2/Al_2O_3 ratio of the zeolite framework and thus the loss of strong acid sites and the formation of meso-pores. The dual functions of the lower acidity strength and the formation of meso-pores lessened coke formation.

3.3. The effect of zeolite USY addition on light olefins selectivity

The effect of the RE-USY zeolite addition to the catalyst on product yields is presented in Table 9. As shown in Table 9, there is a significant increase in ethylene and propylene production when the RE-USY zeolite was added. The yields of C_2–C_3 light olefins showed a volcano trend with the increasing amount of large pore zeolite added and the maximum total yields of ethylene and propylene reached to 24.5 wt% when 20 wt% ZSM-5 zeolite and 20 wt% RE-USY zeolite were used as active components in the catalyst, with the ethylene and propylene yield being increased by 9.2 wt% compared with that (15.3 wt%) of a catalyst containing only the ZSM-5 zeolite as active component.

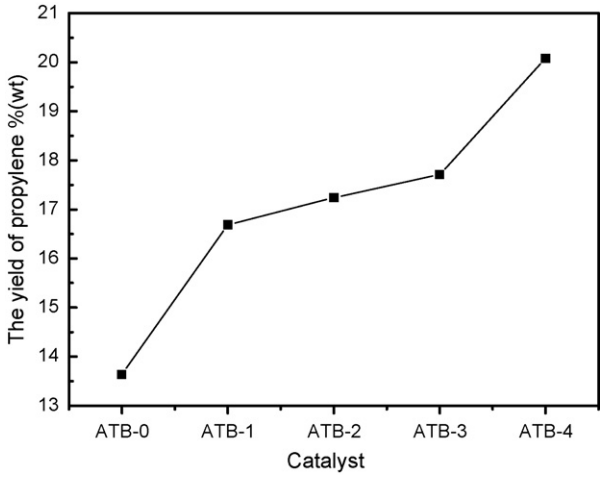

Fig. 6. The variation in the propylene yield of the catalysts containing different AT-Hβ zeolite additions.

Table 9
Product yields (wt%) on the Y catalyst series

Product yields	Catalyst				
	Y-0	Y-1	Y-2	Y-3	Y-4
Dry gas	10.8	11.0	13.7	12.6	12.0
Liquid gas	37.3	42.1	44.2	33.9	37.2
Liquid	44.3	39.6	34.1	45.9	41.8
Coke	7.5	7.3	8.1	7.6	9.0
Ethylene	4.6	5.0	6.7	5.5	5.9
Propylene	10.7	16.3	17.8	16.0	15.3
Ethylene + propylene	15.3	21.3	24.5	21.5	21.2

As it is well known, two cracking steps must be involved to obtain light olefins from heavy oil cracking. First, a catalyst component that is either a large pore zeolite or an active amorphous matrix or their combination cracks the feed into naphtha range hydrocarbons; second, a catalyst component that is a medium or small pore zeolite cracks the naphtha range hydrocarbons into light olefins. The medium or small pore zeolite cannot directly crack the large hydrocarbon molecules in the feed. Hence, it is concerned that adding excessive medium or small pore zeolite into the catalyst could unduly dilute the amorphous or large pore catalytic component and thus restrain the first step of cracking the FCC feed into naphtha range hydrocarbons, therefore the yield of light olefins was very low (15.3 wt%) when using the catalyst containing only the ZSM-5 zeolite as active component. Similarly, a higher content of the large pore zeolites in the catalyst could unduly dilute the medium or small pore catalytic component to restrain the second step of cracking the naphtha range hydrocarbons into light olefins, therefore the yield of light olefins would be also

Table 10
Product yields (wt%) on the B catalyst series

Product yields	Catalyst				
	B-0	B-1	B-2	B-3	B-4
Dry gas	10.8	14.0	12.4	14.4	14.8
Liquid gas	37.3	45.3	40.7	39.8	35.2
Gasoline	–	–	26.1	–	–
Diesel	–	–	9.0	–	–
Heavy oil	–	–	5.5	–	–
Coke	7.5	5.6	6.3	6.8	7.3
Ethylene	4.6	7.8	6.6	6.3	6.5
Propylene	10.7	17.1	20.1	15.6	13.0
Ethylene + propylene	15.3	24.9	26.7	21.9	19.5
Conversion (HCO)	–	–	94.5	–	–

Note: "–" indicates that the composition of liquid was not analyzed.

Table 11
Compositions of the "pure zeolite" catalysts

Catalyst	B-2	B-4
Zeolite (wt%)		
HZSM-5	20	–
AT-Hβ-4	20	40
Kaolin (wt%)	45	45
Alumina binder (wt%)	15	15
Catalyst	Z-2	Z-4
Zeolite (wt%)		
HZSM-5	5	–
AT-Hβ-4	5	10
Quartz sands (wt%)	90	90

Table 12
Product yields (wt%) on the "pure zeolite" catalysts

Product yields	Catalyst			
	B-2	B-4	Z-2	Z-4
Dry gas	12.4	14.8	10.6	12.1
Liquid gas	40.7	35.2	23.0	14.9
Liquid	40.6	42.7	65.1	71.8
Coke	6.3	7.3	1.3	1.3
Ethylene	6.6	6.5	5.4	5.6
Propylene	20.1	13.0	12.4	8.1
Ethylene + propylene	26.7	19.5	17.7	13.7

low. Such an example is the catalyst containing only the RE-USY zeolite as active component, which produced only 21.2 wt% light olefins. Therefore, an optimum combination of a ZSM-5 zeolite and a large pore zeolite (such as the RE-USY zeolite) as active components can favor a high light olefins yield. Moreover, the data listed in Table 9 show that catalysts Y-0 to Y-4 have no obvious difference in their coke yield, possibly because the changes in light olefins yields were resulted from the pore structure rather than from the activity enhancement. Their similar temperature programmed desorption of ammonia (NH_3-TPD) profiles support this point of view.

3.4. The effect of zeolite β on light olefins selectivity

To know the effect of the zeolite β addition on light olefins selectivity, one alkali-treated Hβ zeolite (AT-Hβ-4) with suitable pore structure (shown in Table 4) and good catalytic performance (shown in Table 8) was chosen as the large pore zeolite. The results of the AT-Hβ-4 zeolite addition into the catalyst on product yields are presented in Table 10.

The data in Table 10 indicate that there is an obvious increase in the yields of ethylene and propylene when the AT-Hβ-4 zeolite was added, and the yields of C_2–C_3 light olefins also show a volcano-shape with the increasing amount of the AT-Hβ-4 zeolite added. The total yield of ethylene and propylene also reached at its maximum (26.7 wt%) when 20 wt% ZSM-5 zeolite and 20 wt% AT-Hβ-4 zeolite were used as active components in the catalyst. Therefore, it can be also concluded that optimum combination of the ZSM-5 and AT-Hβ zeolite addition plays an important role in increasing the yields of C_2–C_3 light olefins. In the present work, 20 wt% ZSM-5 zeolite and 20 wt% large pore zeolite can be considered as an optimum combination, at which the naphtha range hydrocarbons produced in the first cracking step over the large pore zeolite can be fairly cracked by the ZSM-5 zeolite in the second cracking step.

The above evaluation results also demonstrate that the ZSM-5 zeolite with large pore zeolite as active components are more effective in increasing the selectivity to light olefins than only ZSM-5 zeolite or large pore zeolite as active component. Moreover, the comparison of Tables 9 and 10 also reveals that the combination of Hβ zeolite and ZSM-5 zeolite is better than that of RE-USY zeolite and ZSM-5 zeolite.

In order to understand the function of "pure zeolite" in the catalyst, two "pure zeolite" catalysts were prepared. They contain 10 wt% zeolite and 90 wt% quartz sands used as diluent, and their compositions are listed in Table 11. The compositions of Cat B-2, Cat B-4 are also listed for comparison. The product yields are presented in Table 12.

In Table 12, it can be seen that the variation in product yield distributions on catalysts B-2 to B-4 is almost consistent with that on catalysts Z-2 to Z-4. Namely, the product yield distributions of the "pure zeolite" catalysts have the same tendency as those of the final catalysts. Moreover, the variation in the textural data of the final catalysts from Cat ATB-1 to ATB-4 (the data are presented in Table 13) is also roughly consistent with that of the pure zeolites from AT-Hβ-1 to AT-Hβ-4 (the data are presented in Table 4). Namely, their external surface areas and pore volumes were all increased, and the mesopore volumes and average pore diameters were also increased. Therefore, the final catalyst can inherit the characteristics of the pure zeolites in certain degree.

4. Conclusion

Comparing the effects of the amount of large pore zeolite added and the pore size of the large pore zeolites, it can be concluded that large pore zeolite addition is an efficient way for increasing the yields of light olefins (ethylene and

Table 13
The textural data of the final catalysts

Catalyst	S_{BET} ($m^2\,g^{-1}$)	S_{micr} ($m^2\,g^{-1}$)	S_{exte} ($m^2\,g^{-1}$)	V_P ($cm^3\,g^{-1}$)	V_{micr} ($cm^3\,g^{-1}$)	V_{meso} ($cm^3\,g^{-1}$)	Average pore diameter (Å)
ATB-1	168	88	80	0.200	0.044	0.156	47.8
ATB-2	168	91	77	0.203	0.045	0.158	48.3
ATB-3	167	85	82	0.209	0.043	0.166	50.1
ATB-4	183	91	91	0.233	0.046	0.187	50.9

propylene), especially propylene. The variation in the yields of C_2–C_3 light olefins presents a volcano-shape along with the increasing amount of large pore zeolite added. The experimental data indicated that 20 wt% of ZSM-5 zeolite and 20 wt% of large pore zeolite as active components is the optimum combination for Daqing heavy oil cracking under the experimental conditions used. When ZSM-5 zeolite and RE-USY zeolite were used as active components, the maximum total yields of ethylene and propylene reached 24.5 wt%, increasing by 9.2 wt% compared with case when using only the ZSM-5 zeolite as active component. Similarly, when the optimum combination of ZSM-5 zeolite and AT-Hβ-4 zeolite was employed, the yield of ethylene and propylene reached 26.7 wt%, increasing by 11.4 wt% compared with the case when using only ZSM-5 zeolite as active component. Moreover, the increase in the pore size of β zeolite also leads to an increase in the yields of light olefins. The present research showed that maximum total yield of ethylene and propylene reached 26.7 wt% when the total pore volume of large pore zeolite added reached the maximum (0.452 $cm^3\ g^{-1}$).

References

[1] Z.T. Li, F.K. Jiang, X.Q. Wang, in: Proceedings of NPRA Annual Meeting, USA, 1990, AM-90-40.
[2] C.Y. Li, Z.T. Li, in: Proceedings of NPRA Annual Meeting, USA, 1994, AM-94-57.
[3] Z.C. Shi, F.M. Zhang, S.H. Liu, US Patent No. 6,211,104 (2001).
[4] J. Biswas, I. Maxwell, Appl. Catal. 63 (1990) 197.
[5] F. Dwyer, T. Degnan, Fluid catalytic cracking: science and technology, studies, in: J. Magee, M. Mitchell (Eds.), Surface Science and Catalysis, vol. 76, Elsevier, Amsterdam, 1993, p. 499.
[6] C.M. Tsang, L.D. Neff, P.E. Dai, US Patent No. 5,472,594 (1995).
[7] Z.C. Shi, W.Y. Shi, Y.F. Ye, X.P. Ge, P. Cao, S.H. Liu, C.G. Xie, Z.T. Li, X.T. Shu, X.M. Yang, W. Fu, M. Zhou, M.Y. He, US Patent No. 5,380,690 (1995).
[8] M. Ke, X.Q. Wang, F.M. Zhang, Petrol. Process. Petrochemicals 34 (2003) 53.
[9] R.R. Xu, Chemistry of Zeolites and Porous Materials, Science Press, Beijing, 2004, p. 250.
[10] M. Ogura, S. Shinomiya, J. Tateno, Y. Nara, M. Nomura, E. Kikuchi, M. Matsukata, Appl. Catal. 219 (2001) 33.
[11] J.S. Jung, J.W. Park, G. Seo, Appl. Catal. 288 (2005) 149.
[12] A.F.H. Wielers, M. Vaarkamp, M.F.M. Post, J. Catal. 127 (1991) 51.
[13] K.A. Cumming, B.W. Wojciechowski, Catal. Rev. Sci. Eng. 38 (1996) 101.
[14] C. Mirodatos, D. Bartomeuf, J. Catal. 67 (1991) 218.